Research Square

Preprints are preliminary reports that have not undergone peer review.
They should not be considered conclusive, used to inform clinical practice,
or referenced by the media as validated information.

Early vitamin B12 treatment mitigates hippocampal neuroinflammation and preserves NeuN-expressing neuron density in a hamster model of post-acute COVID-19

Marina da Silva Oliveira
Neurogenômica, Instituto René Rachou (IRR), Fundação Oswaldo Cruz (Fiocruz)
Leonardo Silva-Contigli
Neurogenômica, Instituto René Rachou (IRR), Fundação Oswaldo Cruz (Fiocruz)
Anna Cristina Matos Salim
Instituto René Rachou (IRR), Fundação Oswaldo Cruz (Fiocruz)
Dayane Lorena Naves de Souza
Neurogenômica, Instituto René Rachou (IRR), Fundação Oswaldo Cruz (Fiocruz)
Natália Satchiko Hojo de Souza
Neurogenômica, Instituto René Rachou (IRR), Fundação Oswaldo Cruz (Fiocruz)
Marco Aurélio Romano-Silva
Universidade Federal de Minas Gerais
Roney Santos Coimbra
roney.coimbra@fiocruz.br

Neurogenômica, Instituto René Rachou (IRR), Fundação Oswaldo Cruz (Fiocruz)

Research Article

Keywords: Post-acute COVID-19, Vitamin B12 therapy, Syrian golden hamster model, CCL11/Eotaxin-1, Hippocampal neuroinflammation

Posted Date: November 5th, 2026

DOI: https://doi.org/10.21203/rs.3.rs-10638786/v1

License: This work is licensed under a Creative Commons Attribution 4.0 International License.
Read Full License

Additional Declarations: No competing interests reported.

Abstract

Cognitive impairment in long COVID has been linked to hippocampal neuroinflammation and elevated levels of CCL11, a chemokine associated with microgliosis and neuronal dysfunction. Vitamin B12 has emerged as a potential modulator of neuroinflammation, including through the inhibition of CCL11 transcription. Adult golden Syrian hamsters were intranasally infected with the SARS-CoV-2 Omicron variant and treated with vitamin B12 beginning three days after infection. Body weight and food intake were monitored throughout the study. At 15 days post infection, hippocampal transcriptomic alterations were investigated by RNA-Seq; microglial density and morphology were assessed by Iba1 immunohistochemistry; and NeuN-expressing postmitotic neuron density and alpha-synuclein levels were evaluated by immunofluorescence in the CA1 and CA3 hippocampal subregions. Plasma vitamin B12 and CCL11 concentrations, as well as hippocampal CCL11 levels, were quantified by ELISA. SARS-CoV-2 infection caused weight loss and reduced food intake during the acute phase and subsequently increased hippocampal CCL11 levels, reduced NeuN+ neuron density, induced sex- and subregion-dependent microglial alterations, and, in females, promoted hippocampal transcriptional reprogramming involving neurodegeneration-related pathways. Vitamin B12 modestly attenuated weight loss, prevented inappetence, and mitigated the increase in hippocampal CCL11 levels. It also preserved NeuN+ neuron density and modulated microglial and transcriptomic alterations in a sex-dependent manner. These findings support a role for CCL11 in hippocampal dysfunction associated with post-acute COVID-19 and suggest that early vitamin B12 treatment may mitigate neuroinflammatory and neuronal alterations, highlighting its potential as an adjuvant therapy for the neurological complications of this disease.

Introduction

Long COVID, also known as post-acute sequelae of SARS-CoV-2 infection (PASC), is characterized by the persistence of symptoms after the resolution of the acute phase of coronavirus disease 2019 (COVID-19). Among these manifestations, cognitive impairment - often described as "brain fog" - has emerged as one of the most frequent and disabling neurological complications (Nalbandian et al. 2021; Davis et al. 2023), with persistent visuoconstructive impairment affecting approximately 25% of patients who had mild COVID-19 (de Paula et al. 2023; Souza-Silva et al. 2024).

Growing evidence implicates neuroinflammation in the pathophysiology of neurological manifestations associated with long COVID. Experimental studies in rodents have demonstrated that SARS-CoV-2 infection can induce persistent microgliosis, impaired neurogenesis, and molecular alterations consistent with neurodegenerative processes in the hippocampus (Käufer et al. 2022; Fernández-Castañeda et al. 2022; Soung et al. 2022). More recently, persistent neuroinflammatory alterations and neuronal dysfunction with parkinsonian features in the brainstem of hamsters up to 80 days after infection were reported (Coleon et al. 2025).

The hippocampus plays a pivotal role in learning, memory, and other cognitive processes and is highly vulnerable to inflammatory insults due to its intense synaptic plasticity and sensitivity to

immunoinflammatory mediators. Neuroinflammatory alterations in this region have been implicated in cognitive decline associated with aging, neurodegenerative diseases, and neurological sequelae induced by viral infections (reviewed in: (Yong et al. 2021; Zhang et al. 2023; Blossom et al. 2025)). In this context, the chemokine C–C motif chemokine ligand 11 (CCL11 or Eotaxin-1) has been identified as a potential mediator linking peripheral immune dysregulation to hippocampal dysfunction. Elevated circulating levels of CCL11 have been associated with impaired neurogenesis, microglial activation, and cognitive decline in both rodents and humans (Villeda et al. 2011; Scabia et al. 2021). Notably, increased plasma levels of CCL11 have been reported in patients with persistent visuoconstructive impairment associated with long COVID (de Paula et al. 2023; Souza-Silva et al. 2024), suggesting the involvement of this chemokine in the neurological sequelae of SARS-CoV-2 infection.

Syrian golden hamsters (*Mesocricetus auratus*) are highly susceptible to SARS-CoV-2 infection and develop predominantly mild and self-limiting acute respiratory disease, similar to non-severe forms of human COVID-19 (Sia et al. 2020). However, experimental infection in these animals induces neuroinflammation and alterations consistent with persistent neurodegenerative processes in the brain. In particular, the accumulation of hyperphosphorylated tau and alpha-synuclein has been demonstrated in neurons of the suprahippocampal cortex 14 days after intranasal infection (Käufer et al. 2022), indicating that pathological processes associated with proteostatic dysfunction may persist beyond the acute phase of infection.

Vitamin B12 has emerged as a potential epidrug - a compound that modulates epigenetic mechanisms - capable of modulating inflammatory pathways associated with neurological disorders. As an essential cofactor for the methionine synthase enzyme in the sulfur amino acid pathway, B12 contributes to the maintenance of cellular methylation reactions by regulating the availability of S-adenosylmethionine (reviewed in: (Cassiano et al. 2023b)). In an infant rat model of pneumococcal meningitis, B12 treatment attenuated microgliosis and apoptosis of postmitotic neurons in the hippocampal dentate gyrus. These protective effects were mediated by DNA methylation-dependent modulation of genes involved in leukocyte recruitment, oxidative stress, and neuroinflammatory pathways (de Queiroz et al. 2020; Cassiano et al. 2023c). Similarly, in whole-blood cultures from patients with moderate or severe COVID-19, B12 acted as an epidrug normalizing the expression of inflammatory and antiviral response genes (Cassiano et al. 2023a). Of particular relevance, B12 increased the methylation of specific CpGs within the 5'-UTR region of *CCL11* in leukocytes from whole-blood cultures of patients with long COVID-associated visuoconstructive impairment, thereby downregulating its transcription (Cassiano et al. 2025).

Based on these observations, it was hypothesized that B12 treatment would attenuate the persistent neuroinflammatory and neurodegeneration-associated alterations in the hippocampus induced by SARS-CoV-2 infection. To test this hypothesis, a Syrian golden hamster model of SARS-CoV-2 infection was used to evaluate plasma and hippocampal CCL11 levels, characterize hippocampal transcriptomic alterations, and assess microglial response and neuronal density changes during the post-acute phase of infection.

Materials and Methods

Animals

Ninety Syrian golden hamsters (48 females and 42 males), aged 8–10 weeks, were obtained from the Production Animal Facility of the René Rachou Institute (Fiocruz, IRR) and transferred to the animal facility of the Biosafety Level 3 Laboratory (BSL-3) at the Federal University of Minas Gerais (UFMG), where they remained until euthanasia. The animals were kept in individual cages, under a 12-hour light/dark cycle, with controlled temperature (20–25°C) and humidity. Water and food were provided *ad libitum* until the day of infection. On the day of infection, a fixed amount of 150 g of food was provided to each animal, without supplementation thereafter until the end of the experiments. This project was approved by the Ethics Committee on the Use of Animals of UFMG (license no. 56/2023).

Infection and treatment

The animals were weighed and anesthetized with a combination of ketamine (200 mg/kg) and xylazine (10 mg/kg), and assigned to two groups, with half of the females and half of the males allocated to each group. The first group was infected with SARS-CoV-2 (Omicron variant; GISAID: EPI_ISL_7699344) intranasally (10^5 PFU in 100 µL of sterile 1x phosphate-buffered saline (PBS)), and the second group received 100 µL of sterile 1x PBS (Sham-infected). After the procedure, the animals were returned to their cages to recover from anesthesia. Starting on the day of infection, the animals were weighed every three days. The amount of feed remaining in each individual cage was weighed on the 15th day post-infection (p.i.). To assess the percentage change in animal body mass throughout the experiment, the weights recorded on days 3, 6, 9, 12, and 15 p.i. were normalized relative to the initial body mass on the day of infection, defined as 100%. To estimate feed consumption per animal, the final weight of the remaining feed in the cage was subtracted from the 150 g offered on the day of infection; then, this value was normalized by the initial weight of the respective animal.

Three days after infection, subcutaneous administration of B12 (0.065 mg/kg diluted in citrate-phosphate buffer, pH 5) was initiated and performed either daily or every three days. The control groups received vehicle alone (citrate-phosphate buffer, pH 5) daily. The animals were assigned to six experimental groups, each comprising eight females or seven males: Sham-infected – Vehicle, Sham-infected – daily vitamin B12, Sham-infected – vitamin B12 every three days, Infected – Vehicle, Infected – daily vitamin B12, and Infected – vitamin B12 every three days. In the groups treated with B12 every three days, the vehicle was administered once daily on the days between B12 administrations.

Sample collection

On day 15 p.i., the animals were weighed and euthanized with a lethal intraperitoneal dose of ketamine (1000 mg/kg) and xylazine (100 mg/kg). After confirmation of the absence of responses to external

stimuli, thoracotomy was performed, and approximately 2 mL of blood was collected by cardiac puncture into heparinized tubes. Samples were centrifuged at 2000 × g for 10 min at 4°C for plasma separation, which was stored at − 20°C for subsequent analyses. Body perfusion was then performed with 50 mL of sterile chilled 1× PBS, pH 7.4, at a flow rate of 500 mL/h. Subsequently, the hippocampus from one cerebral hemisphere was dissected and stored in RNAlater (Sigma-Aldrich, Saint Louis, MO) at 4°C overnight and then at − 80°C. The other hemisphere was post-fixed in 4% paraformaldehyde (PFA), dehydrated through increasing concentrations of ethanol and xylene, and subsequently embedded in paraffin for immunohistochemical and immunofluorescence analyses.

Extraction of proteins and RNA from hippocampal tissue

Protein lysates and total RNA were extracted from the same hippocampal samples preserved in RNAlater using the PARIS Kit (Invitrogen, Carlsbad, CA). The RNA concentration was determined by fluorimetry using the Qubit RNA HS Assay Kit and the Qubit 2.0 Fluorometer (Invitrogen). Protein lysates and RNA samples were stored at − 80°C.

Quantification of vitamin B12 and CCL11

Plasma B12 levels were quantified using the Vitamin B12 ELISA Kit (Abcam, Cambridge, UK). CCL11 protein levels were quantified in plasma and hippocampal protein lysates using the Hamster Eotaxin-1 (ETN1) ELISA Kit (MyBioSource, San Diego, CA, USA). CCL11 concentrations in the hippocampal protein lysates were normalized to the total protein concentration of the respective samples, determined using the Pierce Bradford Protein Assay Kit (Thermo Fisher Scientific, Waltham, MA, USA).

RNA sequencing (RNA-Seq) and Bioinformatics

Four hippocampal RNA samples from females and four from males in each experimental group of interest were used for cDNA library construction with the TruSeq Stranded mRNA Kit (Illumina, San Diego, CA, USA). Indexed libraries were sequenced on the NextSeq 2000 platform using the P2 Reagents Kit (100 cycles) (Illumina). The obtained reads were processed with Trimmomatic (Bolger et al. 2014) to remove low-quality bases and reads shorter than 36 nt. The remaining reads were then mapped to the *M. auratus* reference genome (GenBank MesAur1.0 assembly) using the Spliced Transcripts Alignment to a Reference (STAR) program (Dobin et al. 2013) with standard parameters and the GSE162208 annotation file from the Gene Expression Omnibus (NCBI) (Nouailles et al. 2021). Data from uniquely mapped reads were normalized by size factors using the median-of-ratios method implemented in the DESeq2 package for R, as previously described (Love et al. 2014), in order to correct for differences in sequencing depth, library throughput, and overall sample composition.

For functional enrichment analysis using Gene Set Enrichment Analysis (GSEA) (Subramanian et al. 2005), human orthologs corresponding to the *M. auratus* genes present in the STAR output files were initially identified using the online tool g:Profiler (https://biit.cs.ut.ee/gprofiler/orth) (Kolberg et al. 2023).

Hamster genes associated with more than one human ortholog, as well as hamster genes sharing the same human ortholog, were subsequently excluded. The files containing normalized data generated by DESeq2 were then edited by replacing the *M. auratus* Ensembl gene IDs with the Human Genome Organisation (HUGO) Gene Nomenclature Committee (HGNC) symbols corresponding to the respective human orthologs. This study evaluated the effects of long COVID by comparing the Infected-Vehicle and Sham-infected - Vehicle groups, as well as the effects of B12 treatment administered every three days in infected animals by comparing the Infected-B12 and Infected - Vehicle groups, on canonical pathways from the Kyoto Encyclopedia of Genes and Genomes (KEGG) database (Kanehisa et al. 2023). The effects of B12 in healthy animals were assessed by comparing the Sham-infected - B12 and Sham-infected - Vehicle groups. GSEA was performed using the following parameters: permutation type, gene set; number of permutations, 1000; metric for ranking genes, Signal2Noise; gene sets database, c2.cp.kegg_legacy.v2024.1.Hs.symbols.gmt; chip platform, Human_Ensembl_Gene_ID_MSigDB.vs.2024.1.Hs.chip; gene set cut-off was FDR < 0.05; all other parameters were kept at their default settings.

Immunohistochemical and immunofluorescence analyses

Coronal brain sections (3 µm thick), collected at approximately Bregma – 2.3 mm, were processed to evaluate the density and branching of Iba1-expressing microglia, the density of NeuN-expressing neurons, and alpha-synuclein levels. For microglial analysis, sections were immunostained using the Novolink Polymer Detection Kit (Leica Biosystems, Nussloch, Germany), according to the manufacturer's instructions. A rabbit monoclonal anti-Iba1 primary antibody (Abcam; ab178847) was used at a dilution of 1:8,000. The sections were then counterstained with hematoxylin. Images of the CA1 and CA3 hippocampal subregions were acquired at 40× magnification using an Aperio Versa scanner (Leica Biosystems) and analyzed using Fiji (ImageJ) (Schindelin et al. 2012). Iba1 + cells were manually counted, and their morphology was assessed by skeleton analysis (Young and Morrison 2018) within 0.3425-mm² rectangular regions of interest (ROIs) positioned at approximately the same location in each image. The analyzed ROIs are schematically illustrated in Fig. 1. Data were expressed as Iba1 + cell density (cells/mm²) and as a microglial branching index, calculated by dividing the ratio of the number of endpoints to the total branch length by the number of Iba1 + cells. Higher branching-index values were interpreted as indicative of a less reactive microglial state.

For the quantification of NeuN+ postmitotic neuron density and total alpha-synuclein levels in ROIs located within the CA1 and CA3 hippocampal subregions, a previously described immunofluorescence protocol for paraffin-embedded sections was employed (Zaqout et al. 2020). The primary antibodies were mouse anti-NeuN (Invitrogen; MA5-33103; 1:1,000 dilution) and rabbit anti-alpha-synuclein (Invitrogen; PA1-18264; 1:500 dilution). Detection was performed using goat anti-mouse IgG conjugated to Alexa Fluor 555 (Invitrogen; A-21422; 1:2,000 dilution) and goat anti-rabbit IgG conjugated to Alexa Fluor 488 (Invitrogen; A-11034; 1:2,000 dilution) secondary antibodies. Images of the CA1 and CA3 hippocampal subregions were acquired at 40× magnification using an EVOS M5000 microscope (Invitrogen) and analyzed using Fiji. ROIs were defined using a 0.0189-mm² rectangle positioned at

approximately the same location in each image, as schematically illustrated in Fig. 1. NeuN+ neurons were manually counted, and the results were expressed as NeuN+ cells/mm². Total alpha-synuclein signal intensity within each ROI was quantified using the Measure function.

Only animals for which intact coronal histological sections were obtained at or near the predefined Bregma coordinate were included in the immunohistochemical and immunofluorescence analyses, with two to three ROIs per animal evaluated from separate, nonconsecutive sections.

Statistical analyses

Statistical analyses were performed using GraphPad Prism software (version 8.0.2) (GraphPad Software Inc., Irvine, CA). Data normality was assessed using the D'Agostino–Pearson and Shapiro–Wilk tests. Comparisons among experimental groups were performed using two-way or three-way ANOVA, followed by Tukey's multiple comparisons test or the two-stage linear step-up procedure of Benjamini, Krieger, and Yekutieli. Pearson's correlation test was used for correlation analyses. Differences were considered statistically significant when *P* or *q* values were less than 0.05.

Detailed information on the ANOVA analyses for each endpoint - including the initial number of animals, the number of outliers or data points outside the interquartile range excluded from each group, degrees of freedom, and F statistics - and on the correlation analyses - including the number of paired samples, *r* values, and 95% confidence intervals - is provided in Online Resource 1.

The experimental design of the study is illustrated in Fig. 1.

Created with BioRender.com

Results

Vitamin B12 attenuates acute clinical manifestations of COVID-19

SARS-CoV-2 infection caused significant body weight loss between days 6 and 9 p.i. (Fig. 2a), as well as reduced food intake (Fig. 2c). Although three-way ANOVA detected no significant main effect of treatment, multiple-comparisons analysis indicated a trend toward attenuated weight loss on day 9 p.i. in infected animals receiving vitamin B12 every three days compared with their vehicle-treated counterparts ($q = 0.0574$; Fig. 2b). Both therapeutic schedules prevented inappetence (Fig. 2c), but daily vitamin B12 administration failed to attenuate body weight loss. Therefore, only the regimen consisting of vitamin B12 administration every three days was included in subsequent analyses. At the end of the experiment, this regimen resulted in a 2.4-fold increase in plasma vitamin B12 levels compared with vehicle-treated control groups (Fig. 2d), regardless of infection status.

On day 15 p.i., infected animals exhibited elevated hippocampal CCL11 levels compared with sham-infected controls. Infected animals treated with B12 showed reduced hippocampal levels of this chemokine compared with infected groups receiving vehicle alone. Furthermore, the data demonstrated a sex-dependent regulation of hippocampal CCL11 levels. Baseline sex differences were observed among vehicle-treated, sham-infected animals, with hippocampal CCL11 levels being 2.25-fold higher in males than in females (mean ± standard deviation: 61.8 ± 18.7 vs. 30.1 ± 9.3; $q = 0.0005$). In the absence of B12 treatment, infection induced a 2.4-fold increase in hippocampal CCL11 levels in females (72.9 ± 8.9 in the Infected - vehicle group vs. 30.1 ± 9.3 in the Sham-infected - vehicle group; $q < 0.0001$) and a 1.34-fold increase in males (82.9 ± 6.8 vs. 61.8 ± 18.7; $q = 0.0138$). Additionally, in the absence of infection, B12 treatment increased hippocampal CCL11 levels by 1.58-fold (97.4 ± 6.5 vs. 61.8 ± 18.7; $q = 0.0004$) in males, an effect not observed in females (Fig. 3a).

In plasma, no baseline sex differences in CCL11 levels were observed, nor were any effects of infection or B12 treatment detected on the levels of this chemokine (Fig. 3b).

Sex-dependent hippocampal transcriptomic alterations during the post-acute phase of COVID-19 and their modulation by vitamin B12

RNA-Seq analysis revealed distinct sex-dependent transcriptional profiles in the hippocampus of infected animals on day 15 p.i.. B12 treatment modulated multiple KEGG pathways, with distinct profiles between females and males.

In the female hippocampus, the Infected - vehicle vs. Sham-infected - vehicle contrast (effect of infection) revealed significant enrichment only in the *Parkinson's disease* and *Oxidative phosphorylation* pathways, both with a Normalized Enrichment Score (NES) > 0, indicating the activation of transcriptional programs associated with neurodegenerative processes and mitochondrial energy metabolism (Fig. 4a). Conversely, the Infected - B12 vs. Infected – Vehicle contrast (effect of B12 treatment in infected animals) revealed significant modulation of a broad set of pathways, predominantly with negative enrichment (NES < 0), indicating inhibition. Among these, the following stand out: a) amino acid metabolism (*Arginine and proline metabolism*, *Phenylalanine metabolism*, *Valine, leucine and isoleucine degradation*); b) DNA replication and repair (*DNA replication*, *Pyrimidine metabolism*); c) immune response (*Antigen processing and presentation*); d) lipid and fatty acid metabolism (*Arachidonic acid metabolism*, *Fatty acid metabolism*, *Propanoate metabolism*); e) mitochondrial energy metabolism (*Citrate cycle TCA cycle*, *Fructose and mannose metabolism*, *Glycolisis gluconeogenesis*, *Oxidative phosphorylation*, *Pyruvate metabolism*); f) neurodegenerative diseases (*Alzheimer's disease*, *Huntington's disease*, *Parkinson's disease*); g) protein synthesis, export and turnover (*Proteasome, Protein export*, *Ribosome*); h) RNA synthesis and processing (*RNA polymerase*, *Spliceosome*) i) redox metabolism (*Glutathione metabolism, Pentose phosphate pathway*, *Peroxisome*). Furthermore, some pathways showed significant positive enrichment, indicating activation in response to B12 treatment, including those related to: a) cell adhesion, organization, interaction, and migration (*ECM receptor interaction*, *Focal adhesion*, *Regulation of actin cytoskeleton*); b) immune response (*Hematopoietic cell lineage*, *JAK-STAT*

signaling pathway); c) intracellular signaling pathways (*mTOR signaling pathway*, *Phosphatidylinositol signaling system*); and d) synaptic plasticity, neuronal signaling (*Axon guidance*, *Calcium signaling pathway*, *ERBB signaling pathway*, *Long term potentiation*) (Fig. 4b). In summary, the infection induced the activation of pathways related to mitochondrial energy metabolism and neurodegenerative diseases in the female hippocampus, whereas B12 treatment exerted the opposite effect by inhibiting these pathways, as well as several others associated with bioenergetic demand, while concomitantly activating pathways related to neuroimmune homeostasis and neuronal plasticity (Online Resource 2).

In the male hippocampus, the Infected - vehicle vs. Sham-infected - vehicle contrast did not reveal significant enrichment in any of the KEGG pathways analyzed. As opposite, the Infected - B12 vs. Infected – Vehicle contrast showed a consistent set of significantly enriched pathways, most of which were activated. Particularly noteworthy were pathways associated with: a) lipid and fatty acid metabolism (*Propanoate metabolism*); b) mitochondrial energy metabolism (*Citrate cycle TCA cycle*, *Oxidative phosphorylation*); c) neurodegenerative diseases (*Parkinson's disease*); and d) protein synthesis (*Ribosome*). The ECM receptor interaction pathway, related to cell adhesion, organization, interaction, and migration, was inhibited by B12 (Fig. 4c). Therefore, in infected males, B12 treatment promoted the activation of pathways related to mitochondrial energy metabolism and neurodegenerative diseases, and bioenergetic demand, while inhibiting neuroimmune homeostasis (Online Resource 2).

Sex-dependent hippocampal transcriptomic alterations induced by vitamin B12 the absence of SARS-CoV-2 infection

In Sham-infected animals, administering B12 every three days promoted markedly sex-dependent transcriptomic changes in the hippocampus. While no significantly enriched KEGG pathways were detected in males, Sham-infected females exhibited activation of pathways associated with: a) intracellular signaling pathways (*Phosphatidylinositol signaling system*); and b) synaptic plasticity and neuronal signaling (*Calcium signaling pathway*, *Hedgehog signaling pathway*, *Long-term depression*, *Long-term potentiation*, *TGF-beta signaling pathway*). Concomitantly, inhibition was detected in pathways associated with: a) DNA replication and repair (*Base excision repair*, *DNA replication*, *Purine metabolism*); b) mitochondrial energy metabolism (*Citrate cycle TCA* cycle, *Oxidative phosphorylation*); c) neurodegenerative diseases (*Alzheimer's disease*, *Huntington's disease*, *Parkinson's disease*); d) protein synthesis and turnover (*Aminoacyl tRNA Biosynthesis*, *Ribosome*, *Proteasome*); f) RNA processing (*Spliceosome*); and g) synaptic plasticity and neuronal signaling (*Neuroactive ligand-receptor interaction*, *Snare interactions in vesicular transport*) (Fig. 4d). This coordinated transcriptional response to B12 in healthy females can be summarized as activation of pathways related to neuronal plasticity, concomitant with inhibition of pathways associated with mitochondrial energy metabolism and neurodegenerative diseases, bioenergetic demand, and selected pathways involved in neuronal plasticity, namely Neuroactive ligand-receptor interaction and SNARE interactions in vesicular transport (Online Resource 2).

Sex- and subregion-dependent hippocampal microglial alterations and their modulation by vitamin B12

In the CA1 and CA3 subregions of the female hippocampus, SARS-CoV-2 infection significantly increased microglial density (Iba1 + cells / mm²) compared with vehicle-treated sham-infected controls. Infection also promoted a shift toward a less ramified, responsive microglial phenotype, as indicated by reduced ((endpoints / branch length) / Iba1 + cells)). In CA1, B12 treatment showed trends toward preventing the infection-associated increases in microglial density (q = 0.0587) and, to a lesser extent, polarization toward a responsive phenotype (q = 0.0735). In the CA3 region, B12 significantly prevented the infection-associated reduction in microglial branching. Unexpectedly, B12 decreased microglial branching in the CA1 of sham-infected females.

Neither infection nor B12 treatment affected microglial outcomes in the CA1 of males. In CA3, however, infection promoted polarization toward a responsive microglial phenotype, whereas B12 reduced microglial density in both infected and sham-infected animals. It is worth noting that, in the absence of infection and B12 treatment, males exhibited higher basal microglial density than females in both the CA1 (37.20 ± 4.28 vs. 29.50 ± 2.25; q = 0.0473) and the CA3 (36.98 ± 2.62 vs. 30.17 ± 0.95; q = 0.0113) (Fig. 5).

Infection-related decrease in hippocampal NeuN+ neuron density and sex- and subregion-dependent modulation of neuronal and alpha-synuclein outcomes by vitamin B12

At 15 days p.i., infection reduced the density of NeuN-expressing postmitotic neurons (NeuN+ cells/mm²) in the CA1 of both females and males (q = 0.0066 and q = 0.0060, respectively), whereas multiple-comparisons analysis indicated a trend toward reduced neuronal density in the CA3 of both sexes (q = 0.0589). Vitamin B12 administration every three days attenuated the infection-associated reduction in NeuN+ neuron density in the CA1 of both females and males (q = 0.0040 and q = 0.0027, respectively) and in the CA3 of females (q = 0.0063). No significant effect of B12 was detected in the CA3 of males. Notably, sham-infected vehicle-treated males exhibited a higher basal density of mature neurons than their female counterparts in the CA1 (2045 ± 126.2 vs. 1720 ± 97.12 NeuN+ cells/mm²; q = 0.0047). After correction for multiple comparisons, neither SARS-CoV-2 infection nor vitamin B12 treatment significantly affected alpha-synuclein levels. However, a nominally significant increase was observed in the CA3 of vitamin B12-treated infected males relative to their vehicle-treated counterparts, supported only by an uncorrected individual P value (P = 0.0290; Fig. 6).

Sex-dependent correlations among hippocampal measures of neuroinflammation, neuronal density, and alpha-synuclein

Possible associations among hippocampal CCL11 levels, measures of microglial response (Iba1 + cell density and branching), NeuN+ neuron density, and total alpha-synuclein levels were evaluated

exclusively in vehicle-treated sham-infected and infected groups. This approach allowed infection-related associations to be examined without the potential influence of vitamin B12 administration. As shown in Fig. 7, females exhibited a broader pattern of significant correlations among hippocampal measures of neuroinflammation, NeuN+ neuron density, and alpha-synuclein levels than males. n females, NeuN+ neuron density correlated positively with microglial branching and negatively with microglial density in both hippocampal subregions. In the CA3, NeuN+ neuron density also correlated negatively with hippocampal CCL11 levels. In both CA1 and CA3, CCL11 levels correlated positively with microglial density; however, these findings should be considered exploratory because data for both parameters were available for only three paired samples in each subregion, precluding the estimation of confidence intervals using Fisher's transformation (Online Resource 1). In contrast, only two significant correlations were identified in males: a negative correlation between microglial density and alpha-synuclein in the CA1, and a positive correlation between microglial branching and NeuN+ neuron density in the CA3.

Discussion

In the present study, SARS-CoV-2 infection was shown to trigger a coordinated response in the hippocampus of golden Syrian hamsters during the early post-acute phase, characterized by increased CCL11 levels, transcriptional reprogramming, increased microglial density, reduced microglial branching, and reduced density of NeuN+ postmitotic neurons. Some of these changes varied according to sex and hippocampal subregion. The main contribution of this work is the demonstration that vitamin B12, administered every three days beginning early in the course of the disease, prevented inappetence during the acute phase of SARS-CoV-2 infection, despite only modestly attenuating weight loss, and mitigated hippocampal alterations detected on day 15 p.i..

One of the main findings of this study was the increase in hippocampal CCL11 levels after the acute phase of infection, which was greater in females and was attenuated by B12 treatment. This vitamin has previously been reported to modulate *CCL11* gene expression by increasing the methylation of specific CpGs within its promoter region (Cassiano et al. 2025). The involvement of CCL11 in the suppression of neurogenesis and in multiple aspects of the pathophysiology of cognitive decline has also been consistently demonstrated (Villeda et al. 2011; Scabia et al. 2021; Fernández-Castañeda et al. 2022). The inverse correlation observed between CCL11 levels and NeuN+ neuron density in females and, more tentatively, the positive correlation between CCL11 levels and Iba1 + cell density - given the small number of paired samples - support the hypothesis that this chemokine may contribute to hippocampal dysfunction during the post-acute phase of SARS-CoV-2 infection. Although the absence of interventions specifically targeting CCL11 or its receptors precludes the establishment of a direct causal relationship, this interpretation is consistent with the findings of Fernández-Castañeda and collaborators (Fernández-Castañeda et al. 2022), who demonstrated in a murine model that mild respiratory SARS-CoV-2 infection is sufficient to induce a persistent increase in cerebrospinal fluid CCL11 levels, even in the absence of detectable viral neuroinvasion. Additionally, these authors reported that systemic administration of CCL11 induces hippocampal microgliosis and reduces neurogenesis. In the hamster model used in the present study, no significant changes in plasma CCL11 levels were detected on day 15 p.i., suggesting

that some aspects of the systemic innate immune response, such as CCL11 expression, may already be undergoing resolution at this stage, in contrast to the persistence of hippocampal alterations. Baseline hippocampal CCL11 levels in males were more than twice those observed in females, whereas the post-acute infection-induced increase in this chemokine was nearly twofold greater in females. Unexpectedly, B12 administration to sham-infected males increased hippocampal CCL11 levels. Together, these findings suggest that sex-dependent regulatory mechanisms - possibly mediated by sex chromosome-linked genes and sex hormones (reviewed in: (Klein and Flanagan 2016)) - distinctly modulate both basal CCL11 levels and its induction in the hippocampus.

Transcriptomic analysis revealed persistent molecular reprogramming during the post-acute phase of SARS-CoV-2 infection, with distinct patterns between males and females. In the hippocampus of females, the post-acute response to infection was characterized by the activation of pathways related to mitochondrial energy metabolism and neurodegeneration, a pattern reversed by B12 treatment. The vitamin also inhibited pathways associated with high bioenergetic demand while activating pathways related to neuroimmune homeostasis and neuronal plasticity. With the caveat that different time points were evaluated, the effects of infection observed in the present study are partially consistent with the neurodegenerative signature described by Coleon and collaborators (Coleon et al. 2025) in the brainstem of hamsters 80 days after infection, characterized by persistent alterations in genes associated with synaptic dysfunction, repression of dopaminergic and glutamatergic receptors, activation of neurodegenerative processes, and reprogramming of energy and mitochondrial metabolism. As reported by these authors, although males and females shared a late transcriptomic signature predominantly associated with synaptic dysfunction and neurodegenerative processes, females exhibited greater impairment in the expression of genes related to synaptic architecture and signaling, whereas males displayed a response more strongly associated with mitochondrial metabolic reprogramming, suggesting partially distinct pathophysiological trajectories during the chronic phase of COVID-19. Unlike the findings reported by Coleon and collaborators (Coleon et al. 2025) in the brainstem 80 days after infection, and in contrast to the pattern observed in females in the present study, the male hippocampus did not exhibit significant modulation of KEGG pathways, including those related to neurodegeneration or mitochondrial energy metabolism, at 15 days p.i.. However, these pathways were activated by B12 treatment in infected animals, suggesting that the effects of B12 on pathways associated with neurodegeneration may depend on both sex and tissue context. Furthermore, the other effects of B12 on the male hippocampal transcriptome were more limited and predominantly associated with metabolic and biosynthetic activation, suggesting increased bioenergetic demand, in contrast to the broad and bidirectional response observed in females.

In the absence of SARS-CoV-2 infection, administering B12 every three days promoted sex-dependent basal effects. In females, coordinated transcriptomic modulation in the hippocampus, predominantly consistent with neuroprotective and homeostatic responses associated with reduced bioenergetic demand, was accompanied by microglial alterations in the CA1 and CA3, suggesting that the treatment regimen may also have induced low-grade neuroimmune activation. These findings raise the possibility that, despite its overall apparently beneficial transcriptional profile, even the every-three-days dosing

regimen may have represented excessive stimulation under physiological conditions in the absence of infection. In contrast, sham-infected males treated with B12 showed no detectable transcriptomic alterations in the hippocampus despite reduced microglial density in the CA3.

Overall, the transcriptomic findings further support previous evidence that B12 regulates gene expression in a pleiotropic manner, predominantly downregulating genes while also upregulating specific subsets (Cassiano et al. 2023c; Cassiano et al. 2023a). A similar profile was previously described in the hippocampus of infant rats with pneumococcal meningitis treated with B12, in which the vitamin promoted methylation of both DNA and histone H3 methylation at lysines 4 and 9 (de Queiroz et al. 2020; Cassiano et al. 2023c), epigenetic marks associated with chromatin opening and condensation, respectively.

Although no individual genes reached adjusted statistical significance and only a few exhibited nominal *P* values < 0.05 in the pairwise DESeq2 contrasts, GSEA - which evaluates the coordinated distribution of predefined gene sets across a ranked gene list rather than relying on significance thresholds for individual genes (Subramanian et al. 2005) - revealed coordinated enrichment of functionally related pathways, consistent with subtle yet biologically organized transcriptional reprogramming.

The transcriptomic alterations observed in the hippocampus of infected animals were accompanied by quantitative and morphological microglial changes consistent with persistent neuroinflammation. The pattern of microglial alterations observed - characterized by increased Iba1 + cell density concomitant with reduced branching complexity - is consistent with the induction of a reactive phenotype during the post-acute response to infection, with modulation dependent on both sex and hippocampal subregion. Equally relevant was the finding that males exhibited higher basal microglial density than females in the CA1 and CA3, indicating the existence of intrinsic sex-dependent differences in hippocampal microglial organization in Syrian golden hamsters, potentially capable of influencing neuroinflammatory responsiveness to infection. This observation is consistent with previous reports of the higher hippocampal microglial density in male mice compared with females (Guneykaya et al. 2018), as well as with evidence of sex-dependent differences in microglial responsiveness to inflammatory stimuli (Villa et al. 2018). Persistent microgliosis following SARS-CoV-2 infection has already been demonstrated in experimental rodent models, even in the absence of detectable neuroinvasion (Käufer et al. 2022; Fernández-Castañeda et al. 2022). However, the present study is the first to demonstrate that the pattern of hippocampal microglial response during the post-acute phase of the infection varies according to both hippocampal subregional organization and sex. These findings partially converge with the report by Coleon and collaborators (Coleon et al. 2025), who demonstrated that only female hamsters infected with SARS-CoV-2 exhibited discrete thalamic microgliosis during the acute phase of infection (4 days p.i.), whereas during the chronic phase (80 days p.i.), a significant increase in microgliosis was observed in the medulla oblongata only in males. In this context, the modulation promoted by B12 - evidenced by the attenuation of parameters associated with microglial response - represents a relevant advance in the search for therapeutic strategies targeting the cerebral manifestations of long COVID. However, the distinct effects of B12 observed between biological sexes and hippocampal subregions suggest that its

action is not limited to nonspecific suppression of microglial activation but rather involves context-dependent mechanisms shaped by the tissue microenvironment. Taken together, these results reinforce the heterogeneous nature of the persistent microglial response following the acute phase of COVID-19 and highlight the importance of considering sex as a biological variable in the evaluation of therapeutic interventions.

Histological correlates of hippocampal transcriptional signatures associated with the activation of neurodegeneration-related pathways were evaluated by measuring NeuN+ neuron density and alpha-synuclein levels. Infection reduced NeuN+ neuron density in the CA1 of both sexes, whereas reductions in the CA3 approached statistical significance in females and males. These findings were partially supported by the transcriptomic data, which revealed activation of neurodegeneration-related pathways exclusively in the female hippocampus following infection. They are also consistent with previous reports linking SARS-CoV-2 infection to impaired hippocampal neurogenesis (Fernández-Castañeda et al. 2022; Soung et al. 2022) and extend these observations by revealing sex-specific transcriptional responses potentially underlying hippocampal neuronal alterations during the post-acute phase of infection. Vitamin B12 administration every three days attenuated the infection-associated reduction in NeuN+ neuron density in the CA1 of both sexes and in the CA3 of females, but not in the CA3 of males. The protective effect observed in females was consistent with the B12-induced attenuation of neurodegeneration-related transcriptional signatures. Furthermore, the present study is the first to demonstrate that the basal densities of NeuN+ postmitotic neurons in the CA1 are higher in males than in females. Neither infection nor B12 significantly altered alpha-synuclein levels after correction for multiple comparisons. Nevertheless, B12-treated infected males exhibited a nominal increase in alpha-synuclein levels in the CA3 compared with their vehicle-treated counterparts, consistent with the transcriptomic evidence of activated neurodegenerative disease-related pathways in these animals.

Previous studies using rodent models of post-acute COVID-19 have identified alterations across several brain regions consistent with neuronal damage or dysfunction. These alterations include reduced neurogenesis, oligodendrocyte loss, myelin dysregulation, and proteostatic alterations characterized by the accumulation of aggregative proteins associated with neurodegeneration (Fernández-Castañeda et al. 2022; Soung et al. 2022). However, among studies using hamster models of SARS-CoV-2 infection, only Käufer and collaborators (Käufer et al. 2022) reported a trend toward reduced NeuN+ neuronal density in the dentate gyrus at 14 days p.i.. Similarly, Ryu and collaborators (Ryu et al. 2024) reported hippocampal neuronal loss associated with microgliosis in a murine model of acute COVID-19, although the affected hippocampal subregions were not specified. More recently, a reduction in the number of tyrosine hydroxylase-expressing cells in the olfactory bulb and substantia nigra was reported in a murine model of post-acute COVID-19. However, these findings should be interpreted with caution, as reduced tyrosine hydroxylase immunostaining may reflect decreased enzyme expression or reduced immunohistochemical signal intensity, rather than actual loss of dopaminergic neurons (Verma et al. 2026). In this context, the present findings extend current understanding of post-acute COVID-19 pathophysiology by demonstrating a significant reduction in NeuN+ neuron density in the CA1 and a similar trend in the CA3 of infected animals as early as 15 days p.i.. However, the extent to which these

findings reflect the neuropathological processes underlying human long COVID remains to be established.

One limitation of the present study is that the presence of SARS-CoV-2 in the hippocampus was not investigated. Most previous studies support the notion that SARS-CoV-2 infection can induce neuroinflammation and reduce neurogenesis beyond the acute phase of the disease, even in the absence of evidence of productive viral replication in the evaluated regions of the central nervous system (Käufer et al. 2022; Fernández-Castañeda et al. 2022; Frere et al. 2022; Soung et al. 2022). More recently, however, Coleon and collaborators (Coleon et al. 2025) reported persistent viral genetic material and productive SARS-CoV-2 replication in the brainstem of hamsters for up to 80 days p.i., associated with neuroinflammation and neuronal dysfunction. Nevertheless, the findings of the present study, interpreted in light of the available literature, support a predominant role for neuroinflammation - rather than direct viral infection - in the pathophysiology of neurological dysfunction associated with long COVID. Consistently, Verma and collaborators (Verma et al. 2026) demonstrated that early anti-inflammatory intervention following SARS-CoV-2 infection is effective in preventing neurological sequelae associated with long COVID. Another limitation of the present study is that only a single time point was evaluated, precluding additional inferences, including those regarding the origin of the CCL11 accumulated in the hippocampus.

Conclusions

SARS-CoV-2 infection triggers a hippocampal neuroinflammatory response that is detectable beyond the acute clinical phase and comprises interrelated molecular and cellular alterations shaped by sex and hippocampal subregion. The present findings indicate that this response is accompanied by reduced postmitotic neuron density. Consistent with previous evidence, the results of this study support the hypothesis that CCL11 contributes to the link between inflammation and neuronal dysfunction in the hippocampus during the post-acute phase of COVID-19. Early pharmacological intervention with vitamin B12 attenuated acute clinical manifestations and post-acute neuroinflammatory changes while preserving postmitotic neuron density, although its effects varied by sex and hippocampal subregion. Overall, these findings support a role for neuroinflammation in the pathophysiology of neurological manifestations associated with post-acute COVID-19, underscore the importance of sex as a biological variable, and provide a rationale for further investigating therapeutic strategies targeting the neuroinflammatory mechanisms potentially associated with cognitive impairment. Given its low cost, broad availability, and generally favorable safety profile, vitamin B12 warrants further investigation as a potential adjuvant therapy for acute clinical manifestations of mild COVID-19 and the neurological complications associated with long COVID.

Declarations

Funding

This work was supported by INOVA FIOCRUZ (VPPCB-005-FIO-20-2-115), the Instituto Nacional de Ciência e Tecnologia em Neurotecnologias Responsáveis (INCT-NeuroTec-R, CNPq grant 406935/2022), and the Rede Mineira de Neuroinflamação (REMINI, FAPEMIG RED-00071-23). LS-C is the recipient of a CNPq undergraduate research scholarship. MSO received a CAPES Master's scholarship.

Competing interests

The authors declare that they have no competing interests.

Ethics approval

This project was approved by the Ethics Committee on the Use of Animals of UFMG (license no. 56/2023).

Animal welfare

All animal procedures were performed in accordance with institutional and national guidelines for the care and use of laboratory animals and were approved by the Ethics Committee on the Use of Animals of UFMG (license no. 56/2023).

Consent to participate

Not applicable.

Consent for publication

Not applicable.

Data availability

The datasets supporting the conclusions of this article are available in the SRA repository [https://www.ncbi.nlm.nih.gov/bioproject/PRJNA1469455].

Acknowledgements

The authors acknowledge the support provided by the Fiocruz Technological Platform Network and by the Fundação de Amparo à Pesquisa do Estado de Minas Gerais through its Integrative Networks program (ReDiPes – APQ-02481-23 and APQ-04991-23) in granting access to core facilities and multi-user laboratories.

Authors' contributions

MSO and LS-C contributed to the execution of the experiments and to data analysis. ACMS, DLNS, and NSHS contributed to the execution of the experiments. MAR-S contributed to data interpretation. RSC conceived the hypothesis and coordinated the study, contributed to the execution of the experiments,

analyzed and interpreted the results, and wrote the manuscript. All authors read and approved the final manuscript. RSC is the guarantor of this work and takes responsibility for the integrity of the study as a whole.

References

1. Blossom V, Ullal SD, D'Souza MM, Ranade AV, Kumar NA, Rai R (2025) Implicating neuroinflammation in hippocampus, prefrontal cortex and amygdala with cognitive deficit: a narrative review. 3 Biotech 15(9):320. https://doi.org/10.1007/s13205-025-04468-2
2. Bolger AM, Lohse M, Usadel B (2014) Trimmomatic: a flexible trimmer for Illumina sequence data. Bioinformatics 30(15):2114–2120. https://doi.org/10.1093/bioinformatics/btu170
3. Cassiano LMG, Cavalcante-Silva V, Oliveira MS, Prado BVO, Cardoso CG, Salim ACM, Franco GR, D'Almeida V, Francisco SC, Coimbra RS (2023a) Vitamin B12 attenuates leukocyte inflammatory signature in COVID-19 via methyl-dependent changes in epigenetic markings. Front Immunol 14:1048790. https://doi.org/10.3389/fimmu.2023.1048790
4. Cassiano LMG, de Paula JJ, Rosa DV, Miranda DM, Romano-Silva MA, Coimbra RS (2025) Vitamin B12 as an epidrug for regulating peripheral blood biomarkers in long COVID-associated visuoconstructive deficit. Sci Rep 15(1):9438. https://doi.org/10.1038/s41598-025-86637-0
5. Cassiano LMG, Oliveira M, da Coimbra S RS (2023b) Vitamin B12 as a neuroprotectant in neuroinflammation. In: Colin Martin V, Preedy P V (eds) Vitamins and Minerals in Neurologic Disorders, 1st edn. Academic, p 812
6. Cassiano LMG, Oliveira MDS, de Queiroz KB, Amancio AMTD, Salim ACM, Fernandes GDR, Carneiro CM, Coimbra RS (2023c) Uncovering the neuroprotective effect of vitamin B12 in pneumococcal meningitis: insights into its pleiotropic mode of action at the transcriptional level. Front Immunol 14:1250055. https://doi.org/10.3389/fimmu.2023.1250055
7. Coleon A, Larrous F, Kergoat L, Tichit M, Hardy D, Obadia T, Kornobis E, Bourhy H, de Melo GD (2025) Hamsters with long COVID present distinct transcriptomic profiles associated with neurodegenerative processes in brainstem. Nat Commun 16(1):6714. https://doi.org/10.1038/s41467-025-62048-7
8. Davis HE, McCorkell L, Vogel JM, Topol EJ (2023) Long COVID: major findings, mechanisms and recommendations. Nat Rev Microbiol 21(3):133–146. https://doi.org/10.1038/s41579-022-00846-2
9. de Paula JJ, Paiva RERP, Souza-Silva NG, Rosa DV, Duran FLS, Coimbra RS, Costa DS, Dutenhefner PR, Oliveira HSD, Camargos ST, Vasconcelos HMM, de Oliveira Carvalho N, da Silva JB, Silveira MB, Malamut C, Oliveira DM, Molinari LC, de Oliveira DB, Januário JN, Silva LC, De Marco LA, Queiroz DMM, Meira W, Busatto G, Miranda DM, Romano-Silva MA (2023) Selective visuoconstructional impairment following mild COVID-19 with inflammatory and neuroimaging correlation findings. Mol Psychiatry 28(2):553–563. https://doi.org/10.1038/s41380-022-01632-5

10. de Queiroz KB, Cavalcante-Silva V, Lopes FL, Rocha GA, D'Almeida V, Coimbra RS (2020) Vitamin B12 is neuroprotective in experimental pneumococcal meningitis through modulation of hippocampal DNA methylation. J Neuroinflammation 17(1):96. https://doi.org/10.1186/s12974-020-01763-y
11. Dobin A, Davis CA, Schlesinger F, Drenkow J, Zaleski C, Jha S, Batut P, Chaisson M, Gingeras TR (2013) STAR: ultrafast universal RNA-seq aligner. Bioinformatics 29(1):15–21. https://doi.org/10.1093/bioinformatics/bts635
12. Fernández-Castañeda A, Lu P, Geraghty AC, Song E, Lee MH, Wood J, O'Dea MR, Dutton S, Shamardani K, Nwangwu K, Mancusi R, Yalçın B, Taylor KR, Acosta-Alvarez L, Malacon K, Keough MB, Ni L, Woo PJ, Contreras-Esquivel D, Toland AMS, Gehlhausen JR, Klein J, Takahashi T, Silva J, Israelow B, Lucas C, Mao T, Peña-Hernández MA, Tabachnikova A, Homer RJ, Tabacof L, Tosto-Mancuso J, Breyman E, Kontorovich A, McCarthy D, Quezado M, Vogel H, Hefti MM, Perl DP, Liddelow S, Folkerth R, Putrino D, Nath A, Iwasaki A, Monje M (2022) Mild respiratory COVID can cause multi-lineage neural cell and myelin dysregulation. Cell 185(14):2452–2468e16. https://doi.org/10.1016/j.cell.2022.06.008
13. Frere JJ, Serafini RA, Pryce KD, Zazhytska M, Oishi K, Golynker I, Panis M, Zimering J, Horiuchi S, Hoagland DA, Møller R, Ruiz A, Kodra A, Overdevest JB, Canoll PD, Borczuk AC, Chandar V, Bram Y, Schwartz R, Lomvardas S, Zachariou V, tenOever BR (2022) SARS-CoV-2 infection in hamsters and humans results in lasting and unique systemic perturbations after recovery. Sci Transl Med 14(664):eabq3059. https://doi.org/10.1126/scitranslmed.abq3059
14. Guneykaya D, Ivanov A, Hernandez DP, Haage V, Wojtas B, Meyer N, Maricos M, Jordan P, Buonfiglioli A, Gielniewski B, Ochocka N, Cömert C, Friedrich C, Artiles LS, Kaminska B, Mertins P, Beule D, Kettenmann H, Wolf SA (2018) Transcriptional and Translational Differences of Microglia from Male and Female Brains. Cell Rep 24(10):2773–2783e6. https://doi.org/10.1016/j.celrep.2018.08.001
15. Kanehisa M, Furumichi M, Sato Y, Kawashima M, Ishiguro-Watanabe M (2023) KEGG for taxonomy-based analysis of pathways and genomes. Nucleic Acids Res 51(D1):D587–D592. https://doi.org/10.1093/nar/gkac963
16. Käufer C, Schreiber CS, Hartke AS, Denden I, Stanelle-Bertram S, Beck S, Kouassi NM, Beythien G, Becker K, Schreiner T, Schaumburg B, Beineke A, Baumgärtner W, Gabriel G, Richter F (2022) Microgliosis and neuronal proteinopathy in brain persist beyond viral clearance in SARS-CoV-2 hamster model. EBioMedicine 79:103999. https://doi.org/10.1016/j.ebiom.2022.103999
17. Klein SL, Flanagan KL (2016) Sex differences in immune responses. Nat Rev Immunol 16(10):626–638. https://doi.org/10.1038/nri.2016.90
18. Kolberg L, Raudvere U, Kuzmin I, Adler P, Vilo J, Peterson H (2023) g:Profiler-interoperable web service for functional enrichment analysis and gene identifier mapping (2023 update). Nucleic Acids Res 51(W1):W207–W212. https://doi.org/10.1093/nar/gkad347
19. Love MI, Huber W, Anders S (2014) Moderated estimation of fold change and dispersion for RNA-seq data with DESeq2. Genome Biol 15(12):550. https://doi.org/10.1186/s13059-014-0550-8

20. Nalbandian A, Sehgal K, Gupta A, Madhavan MV, McGroder C, Stevens JS, Cook JR, Nordvig AS, Shalev D, Sehrawat TS, Ahluwalia N, Bikdeli B, Dietz D, Der-Nigoghossian C, Liyanage-Don N, Rosner GF, Bernstein EJ, Mohan S, Beckley AA, Seres DS, Choueiri TK, Uriel N, Ausiello JC, Accili D, Freedberg DE, Baldwin M, Schwartz A, Brodie D, Garcia CK, Elkind MSV, Connors JM, Bilezikian JP, Landry DW, Wan EY (2021) Post-acute COVID-19 syndrome. Nat Med 27(4):601–615. https://doi.org/10.1038/s41591-021-01283-z
21. Nouailles G, Wyler E, Pennitz P, Postmus D, Vladimirova D, Kazmierski J, Pott F, Dietert K, Muelleder M, Farztdinov V, Obermayer B, Wienhold SM, Andreotti S, Hoefler T, Sawitzki B, Drosten C, Sander LE, Suttorp N, Ralser M, Beule D, Gruber AD, Goffinet C, Landthaler M, Trimpert J, Witzenrath M (2021) Temporal omics analysis in Syrian hamsters unravel cellular effector responses to moderate COVID-19. Nat Commun 12(1):4869. https://doi.org/10.1038/s41467-021-25030-7
22. Ryu JK, Yan Z, Montano M, Sozmen EG, Dixit K, Suryawanshi RK, Matsui Y, Helmy E, Kaushal P, Makanani SK, Deerinck TJ, Meyer-Franke A, Rios Coronado PE, Trevino TN, Shin MG, Tognatta R, Liu Y, Schuck R, Le L, Miyajima H, Mendiola AS, Arun N, Guo B, Taha TY, Agrawal A, MacDonald E, Aries O, Yan A, Weaver O, Petersen MA, Meza Acevedo R, Alzamora MDPS, Thomas R, Traglia M, Kouznetsova VL, Tsigelny IF, Pico AR, Red-Horse K, Ellisman MH, Krogan NJ, Bouhaddou M, Ott M, Greene WC, Akassoglou K (2024) Fibrin drives thromboinflammation and neuropathology in COVID-19. Nature 633(8031):905–913. https://doi.org/10.1038/s41586-024-07873-4
23. Scabia G, Testa G, Scali M, Del Turco S, Desiato G, Berardi N, Sale A, Matteoli M, Maffei L, Maffei M, Mainardi M, Consortium (2021) Reduced ccl11/eotaxin mediates the beneficial effects of environmental stimulation on the aged hippocampus. Brain Behav Immun 98:234–244. https://doi.org/10.1016/j.bbi.2021.08.222
24. Schindelin J, Arganda-Carreras I, Frise E, Kaynig V, Longair M, Pietzsch T, Preibisch S, Rueden C, Saalfeld S, Schmid B, Tinevez JY, White DJ, Hartenstein V, Eliceiri K, Tomancak P, Cardona A (2012) Fiji: an open-source platform for biological-image analysis. Nat Methods 9(7):676–682. https://doi.org/10.1038/nmeth.2019
25. Sia SF, Yan LM, Chin AWH, Fung K, Choy KT, Wong AYL, Kaewpreedee P, Perera RAPM, Poon LLM, Nicholls JM, Peiris M, Yen HL (2020) Pathogenesis and transmission of SARS-CoV-2 in golden hamsters. Nature 583(7818):834–838. https://doi.org/10.1038/s41586-020-2342-5
26. Soung AL, Vanderheiden A, Nordvig AS, Sissoko CA, Canoll P, Mariani MB, Jiang X, Bricker T, Rosoklija GB, Arango V, Underwood M, Mann JJ, Dwork AJ, Goldman JE, Boon ACM, Boldrini M, Klein RS (2022) COVID-19 induces CNS cytokine expression and loss of hippocampal neurogenesis. Brain 145(12):4193–4201. https://doi.org/10.1093/brain/awac270
27. Souza-Silva NG, Rosa DV, de Paula JJ, Coimbra RS, Miranda DM, Romano-Silva MA (2024) Follow-up of cognitive impairment and inflammatory profile in individuals with mild COVID-19. J Neuroimmunol 389:578327. https://doi.org/10.1016/j.jneuroim.2024.578327
28. Subramanian A, Tamayo P, Mootha VK, Mukherjee S, Ebert BL, Gillette MA, Paulovich A, Pomeroy SL, Golub TR, Lander ES, Mesirov JP (2005) Gene set enrichment analysis: a knowledge-based

approach for interpreting genome-wide expression profiles. Proc Natl Acad Sci U S A 102(43):15545–15550. https://doi.org/10.1073/pnas.0506580102

29. Verma AK, Tan L, Schuster N, Moye SL, Lin LC, Lowery S, Duraisami E, Lloréns JEA, Qiu Q, Hefti M, Meyerholz DK, Coleman MC, Yu CR, Albers MW, Perlman S (2026) Combination antiviral and anti-inflammatory therapy mitigates persistent neurological deficits in mice post SARS-CoV-2 infection. Proc Natl Acad Sci U S A 123(2):e2530209123. https://doi.org/10.1073/pnas.2530209123
30. Villa A, Gelosa P, Castiglioni L, Cimino M, Rizzi N, Pepe G, Lolli F, Marcello E, Sironi L, Vegeto E, Maggi A (2018) Sex-Specific Features of Microglia from Adult Mice. Cell Rep 23(12):3501–3511. https://doi.org/10.1016/j.celrep.2018.05.048
31. Villeda SA, Luo J, Mosher KI, Zou B, Britschgi M, Bieri G, Stan TM, Fainberg N, Ding Z, Eggel A, Lucin KM, Czirr E, Park JS, Couillard-Després S, Aigner L, Li G, Peskind ER, Kaye JA, Quinn JF, Galasko DR, Xie XS, Rando TA, Wyss-Coray T (2011) The ageing systemic milieu negatively regulates neurogenesis and cognitive function. Nature 477(7362):90–94. https://doi.org/10.1038/nature10357
32. Yong SJ, Yong MH, Teoh SL, Soga T, Parhar I, Chew J, Lim WL (2021) The Hippocampal Vulnerability to Herpes Simplex Virus Type I Infection: Relevance to Alzheimer's Disease and Memory Impairment. Front Cell Neurosci 15:695738. https://doi.org/10.3389/fncel.2021.695738
33. Young K, Morrison H (2018) Quantifying Microglia Morphology from Photomicrographs of Immunohistochemistry Prepared Tissue Using ImageJ. J Vis Exp. https://doi.org/10.3791/57648
34. Zaqout S, Becker LL, Kaindl AM (2020) Immunofluorescence Staining of Paraffin Sections Step by Step. Front Neuroanat 14:582218. https://doi.org/10.3389/fnana.2020.582218
35. Zhang W, Xiao D, Mao Q, Xia H (2023) Role of neuroinflammation in neurodegeneration development. Signal Transduct Target Ther 8(1):267. https://doi.org/10.1038/s41392-023-01486-5

Figures

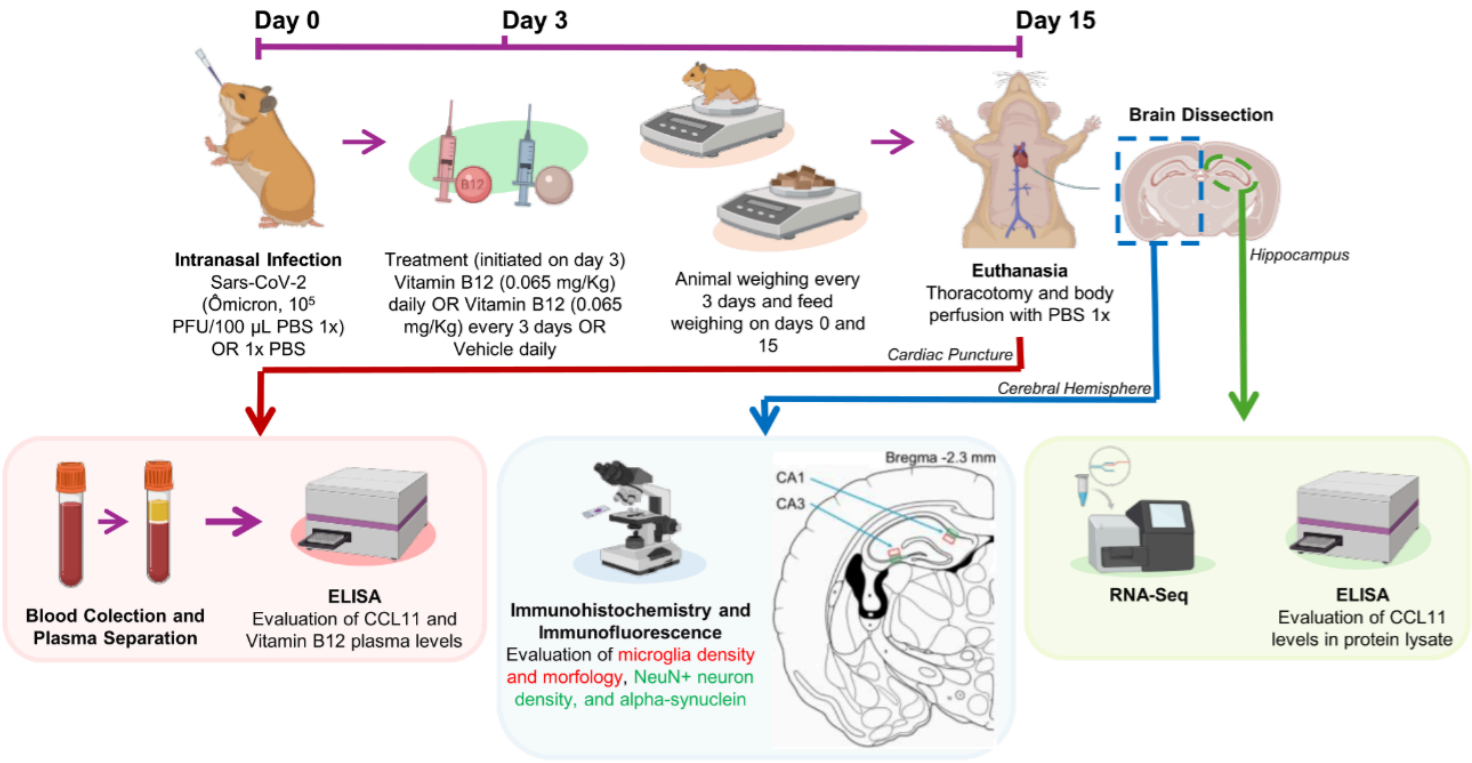
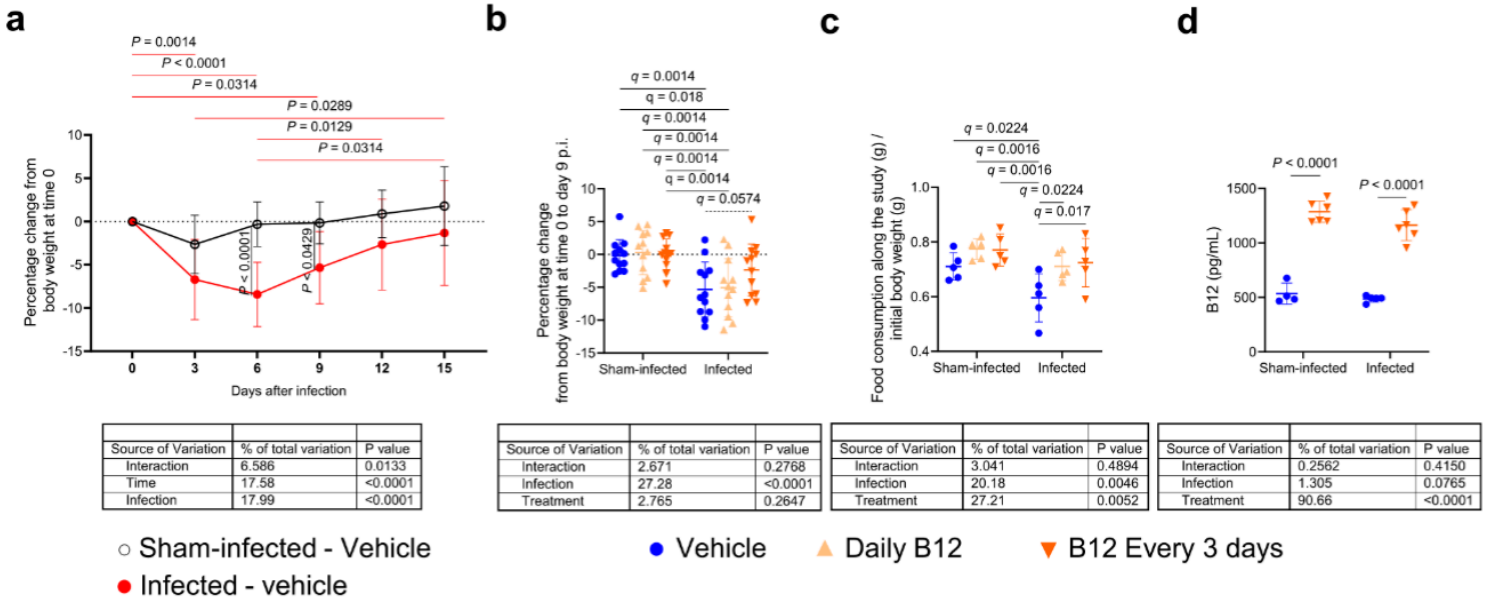


Figure 1

Experimental design

Created with BioRender.com



Source of Variation	% of total variation	P value
Interaction	6.586	0.0133
Time	17.58	<0.0001
Infection	17.99	<0.0001

Source of Variation	% of total variation	P value
Interaction	2.671	0.2768
Infection	27.28	<0.0001
Treatment	2.765	0.2647

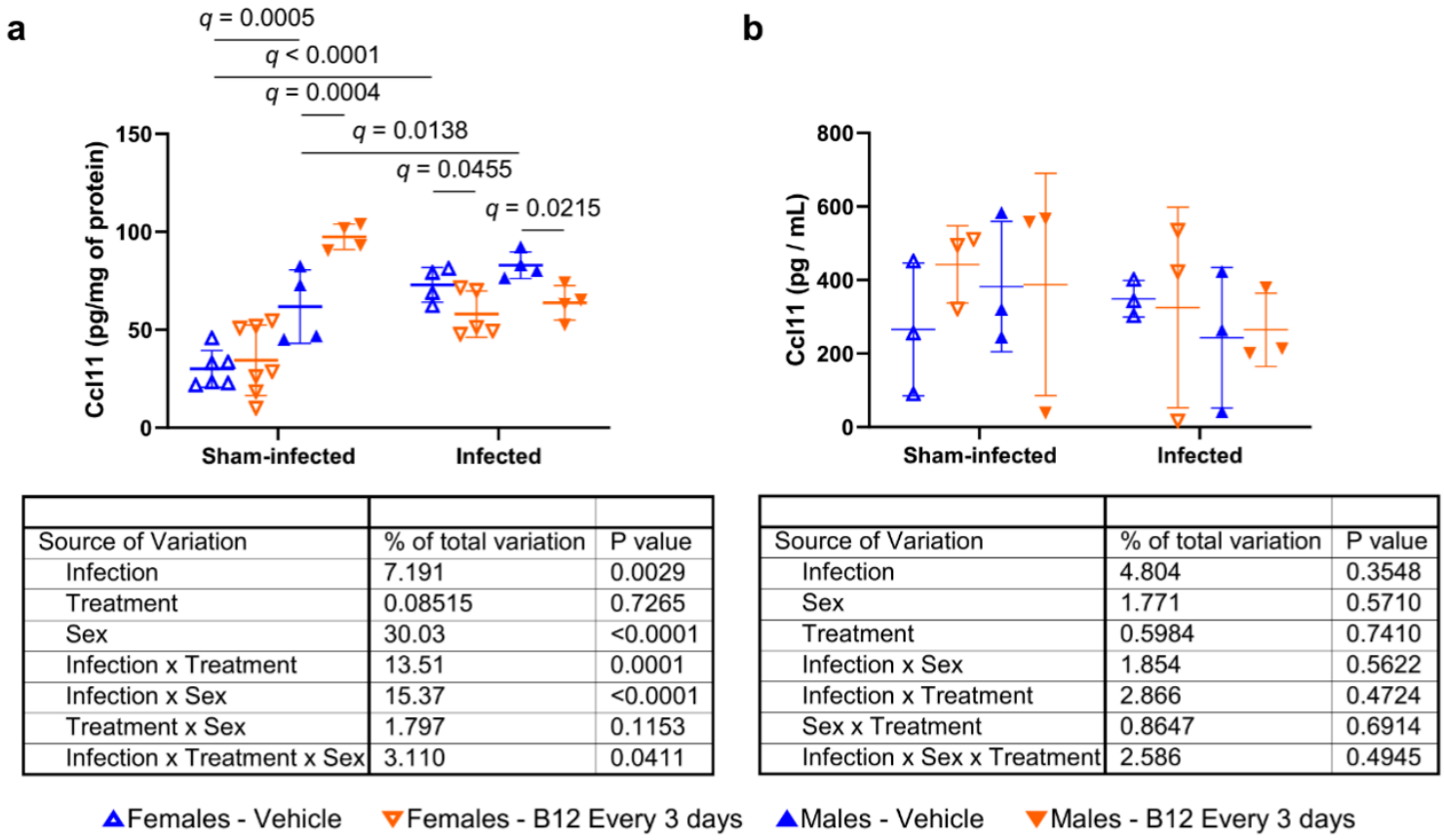
Source of Variation	% of total variation	P value
Interaction	3.041	0.4894
Infection	20.18	0.0046
Treatment	27.21	0.0052

Source of Variation	% of total variation	P value
Interaction	0.2562	0.4150
Infection	1.305	0.0765
Treatment	90.66	<0.0001

Figure 2

Clinical outcomes and plasma vitamin B12 levels following treatment

(a) Variation in body weight throughout the experiment in response to infection without vitamin B12 treatment (12 animals per group). Red horizontal bars indicate differences over time within the infected animals. **(b)** Effects of infection and vitamin B12 therapeutic regimens on body weight loss observed on the ninth day p.i.. **(c)** Effects of infection and vitamin B12 therapeutic regimens on inappetence. **(d)** Plasma B12 levels at the end of the experiment (15th day p.i.). Statistical analyses were performed using two-way ANOVA followed by multiple-comparisons with Tukey's test **(a**, **d)** or Two-stage linear step-up procedure of Benjamini, Krieger and Yekutieli **(b**, **c)**. Data are presented as mean and standard deviation. In panel **C**, data out of the interquartile range were excluded. One outlier was excluded from panel **d** using the ROUT test, Q = 10%



Source of Variation	% of total variation	P value
Infection	7.191	0.0029
Treatment	0.08515	0.7265
Sex	30.03	<0.0001
Infection x Treatment	13.51	0.0001
Infection x Sex	15.37	<0.0001
Treatment x Sex	1.797	0.1153
Infection x Treatment x Sex	3.110	0.0411

Source of Variation	% of total variation	P value
Infection	4.804	0.3548
Sex	1.771	0.5710
Treatment	0.5984	0.7410
Infection x Sex	1.854	0.5622
Infection x Treatment	2.866	0.4724
Sex x Treatment	0.8647	0.6914
Infection x Sex x Treatment	2.586	0.4945

Figure 3

CCL11 protein levels

(a) Hippocampus; **(b)** Plasma. Three-way ANOVA and Two-stage linear step-up procedure of Benjamini, Krieger and Yekutieli for multiple comparisons. Data are presented as means and standard deviations. Outliers were excluded with Grubbs test, alpha = 0.2

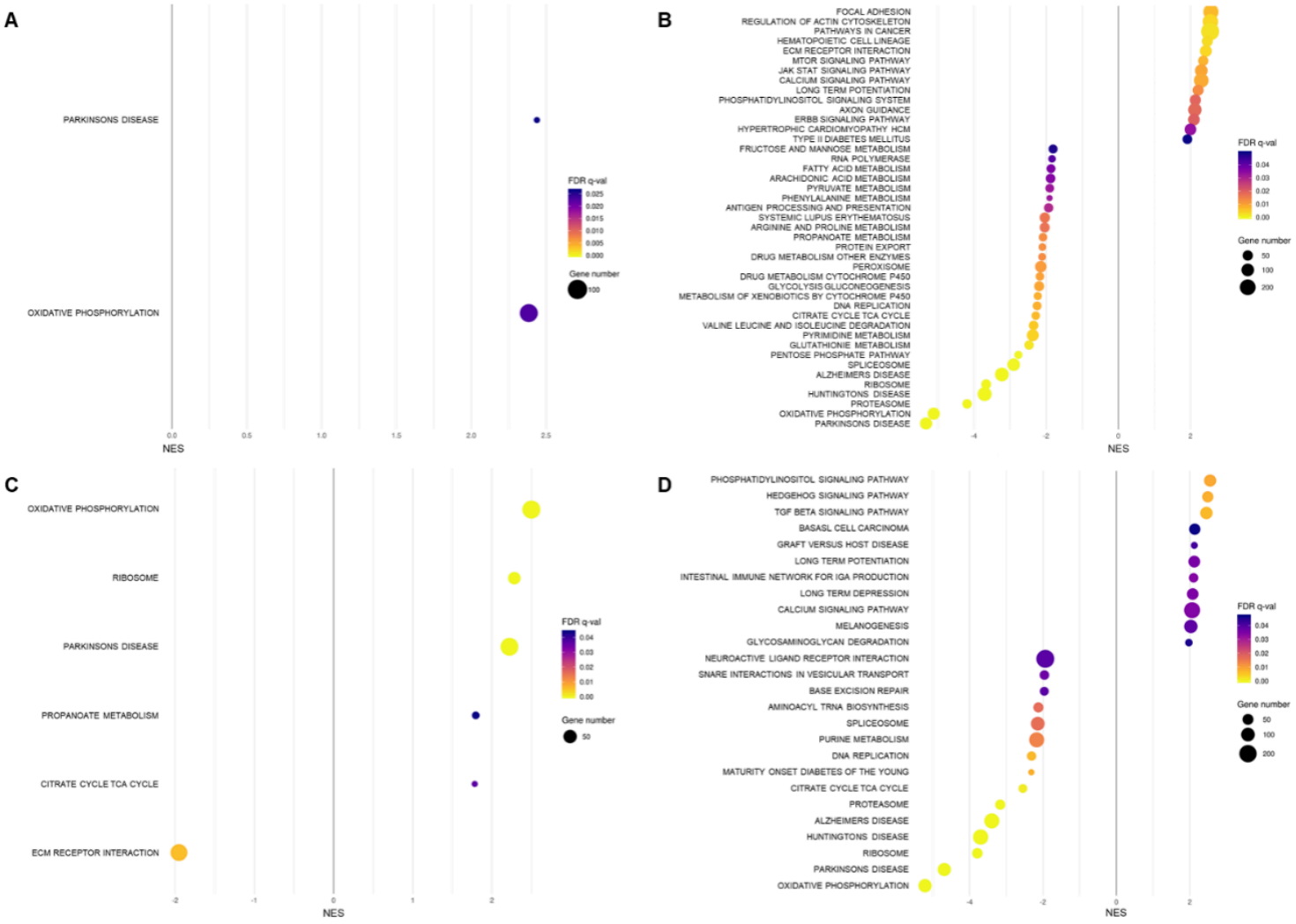
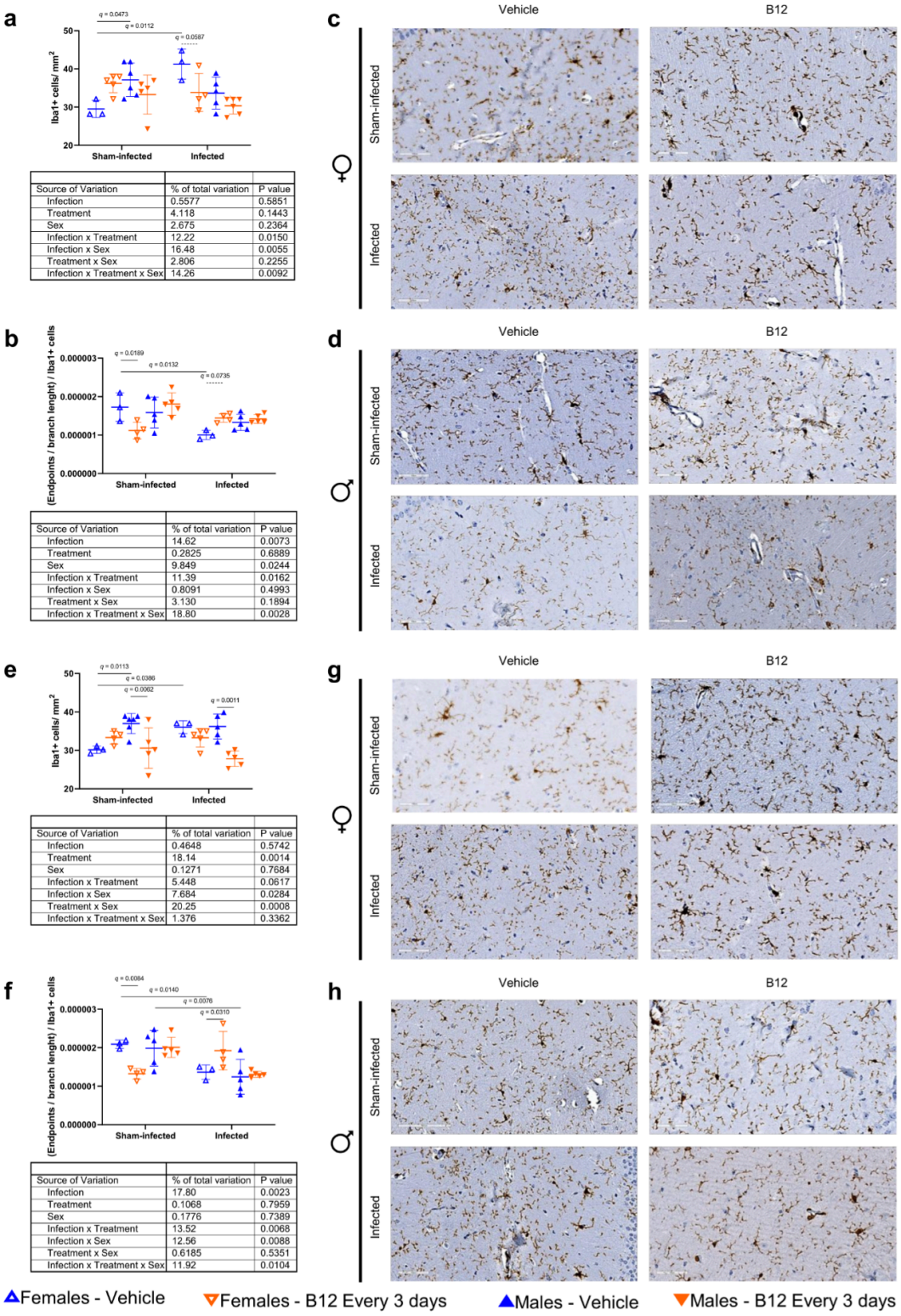


Figure 4

Effects of SARS-CoV-2 infection and vitamin B12 treatment on hippocampal transcriptional signatures revealed by KEGG pathway enrichment analysis

(a) Infected - vehicle vs. Sham-infected – Vehicle, females. **(b)** Infected - B12 every 3 days vs. Infected – Vehicle, females. **(c)** Infected - B12 every 3 days vs. Infected - vehicle, males. **(d)** Sham-infected - B12 every 3 days vs. Sham-infected – Vehicle, females. NES: normalized enrichment score. Statistical significance threshold: FDR < 0.05



Source of Variation	% of total variation	P value
Infection	0.5577	0.5851
Treatment	4.118	0.1443
Sex	2.675	0.2364
Infection x Treatment	12.22	0.0150
Infection x Sex	16.48	0.0055
Treatment x Sex	2.806	0.2255
Infection x Treatment x Sex	14.26	0.0092

Source of Variation	% of total variation	P value
Infection	14.62	0.0073
Treatment	0.2825	0.6889
Sex	9.849	0.0244
Infection x Treatment	11.39	0.0162
Infection x Sex	0.8091	0.4993
Treatment x Sex	3.130	0.1894
Infection x Treatment x Sex	18.80	0.0028

Source of Variation	% of total variation	P value
Infection	0.4648	0.5742
Treatment	18.14	0.0014
Sex	0.1271	0.7684
Infection x Treatment	5.448	0.0617
Infection x Sex	7.684	0.0284
Treatment x Sex	20.25	0.0008
Infection x Treatment x Sex	1.376	0.3362

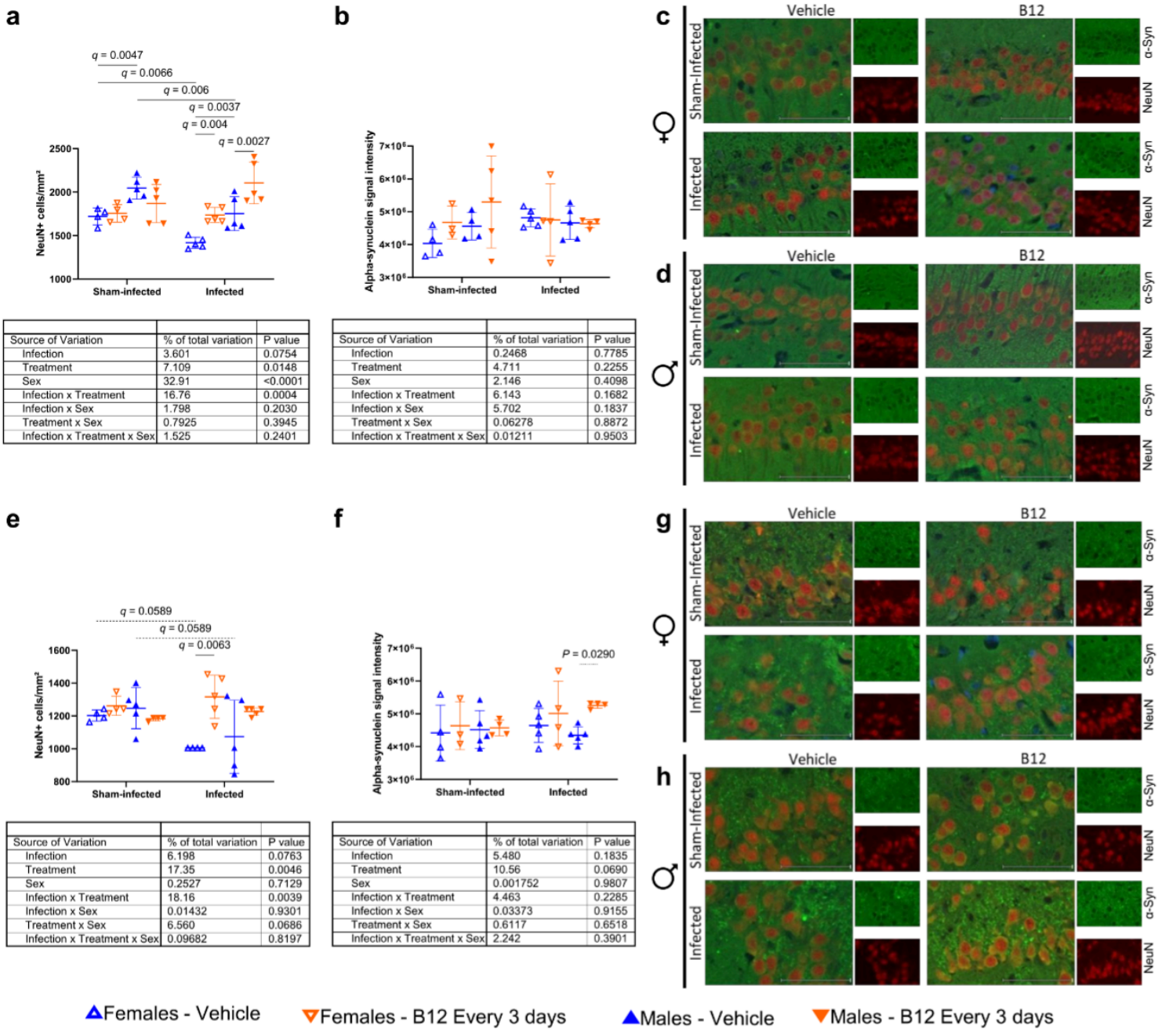
Source of Variation	% of total variation	P value
Infection	17.80	0.0023
Treatment	0.1068	0.7959
Sex	0.1776	0.7389
Infection x Treatment	13.52	0.0068
Infection x Sex	12.56	0.0088
Treatment x Sex	0.6185	0.5351
Infection x Treatment x Sex	11.92	0.0104

Figure 5

Effects of SARS-CoV-2 infection and vitamin B12 treatment on hippocampal microglia

(a-d) CA1; **(e-h)** CA3. Microgliosis was assessed based on Iba1+ cell density (Iba1+ cells/ mm²) **(a**, **e)** and by microglial branching complexity ((endpoints / branch length) / Iba1+ cells)) **(b**, **f)**. Data outside of the interquartile range were excluded. Statistical analyses were performed using three-way ANOVA followed by the Benjamini, Krieger, and Yekutieli multiple-comparisons test. Data are presented as mean

and standard deviation. Dashed lines indicate *q*-values approaching statistical significance. Representative images of CA1 **(c**, **d)** and **(g**, **h)** CA3, acquired at 40× magnification. White horizontal bars = 100 µm



Source of Variation	% of total variation	P value
Infection	3.601	0.0754
Treatment	7.109	0.0148
Sex	32.91	<0.0001
Infection x Treatment	16.76	0.0004
Infection x Sex	1.798	0.2030
Treatment x Sex	0.7925	0.3945
Infection x Treatment x Sex	1.525	0.2401

Source of Variation	% of total variation	P value
Infection	0.2468	0.7785
Treatment	4.711	0.2255
Sex	2.146	0.4098
Infection x Treatment	6.143	0.1682
Infection x Sex	5.702	0.1837
Treatment x Sex	0.06278	0.8872
Infection x Treatment x Sex	0.01211	0.9503

Source of Variation	% of total variation	P value
Infection	6.198	0.0763
Treatment	17.35	0.0046
Sex	0.2527	0.7129
Infection x Treatment	18.16	0.0039
Infection x Sex	0.01432	0.9301
Treatment x Sex	6.560	0.0686
Infection x Treatment x Sex	0.09682	0.8197

Source of Variation	% of total variation	P value
Infection	5.480	0.1835
Treatment	10.56	0.0690
Sex	0.001752	0.9807
Infection x Treatment	4.463	0.2285
Infection x Sex	0.03373	0.9155
Treatment x Sex	0.6117	0.6518
Infection x Treatment x Sex	2.242	0.3901

Figure 6

Effects of SARS-CoV-2 infection and vitamin B12 treatment on neuronal density and alpha-synuclein accumulation in the hippocampus

(a-d) CA1 and **(e-h)** CA3. Mature neuron density was estimated as NeuN+ cells/mm² (red channel). Alpha-synuclein levels were estimated from green-channel signal intensity. Statistical analyses were performed using three-way ANOVA followed by multiple-comparison testing with the Two-stage linear step-up procedure of Benjamini, Krieger and Yekutieli. Data are presented as mean and standard

deviation. Outliers were removed using Grubbs' test (alpha = 0.2). Dashed lines indicate *q* values approaching statistical significance, whereas dotted lines indicate nominal *P* values unadjusted for multiple comparisons. Representative images of CA1 **(c**, **d)** and **(g**, **h)** CA3, acquired at 40× magnification. White horizontal bars = 75 µm

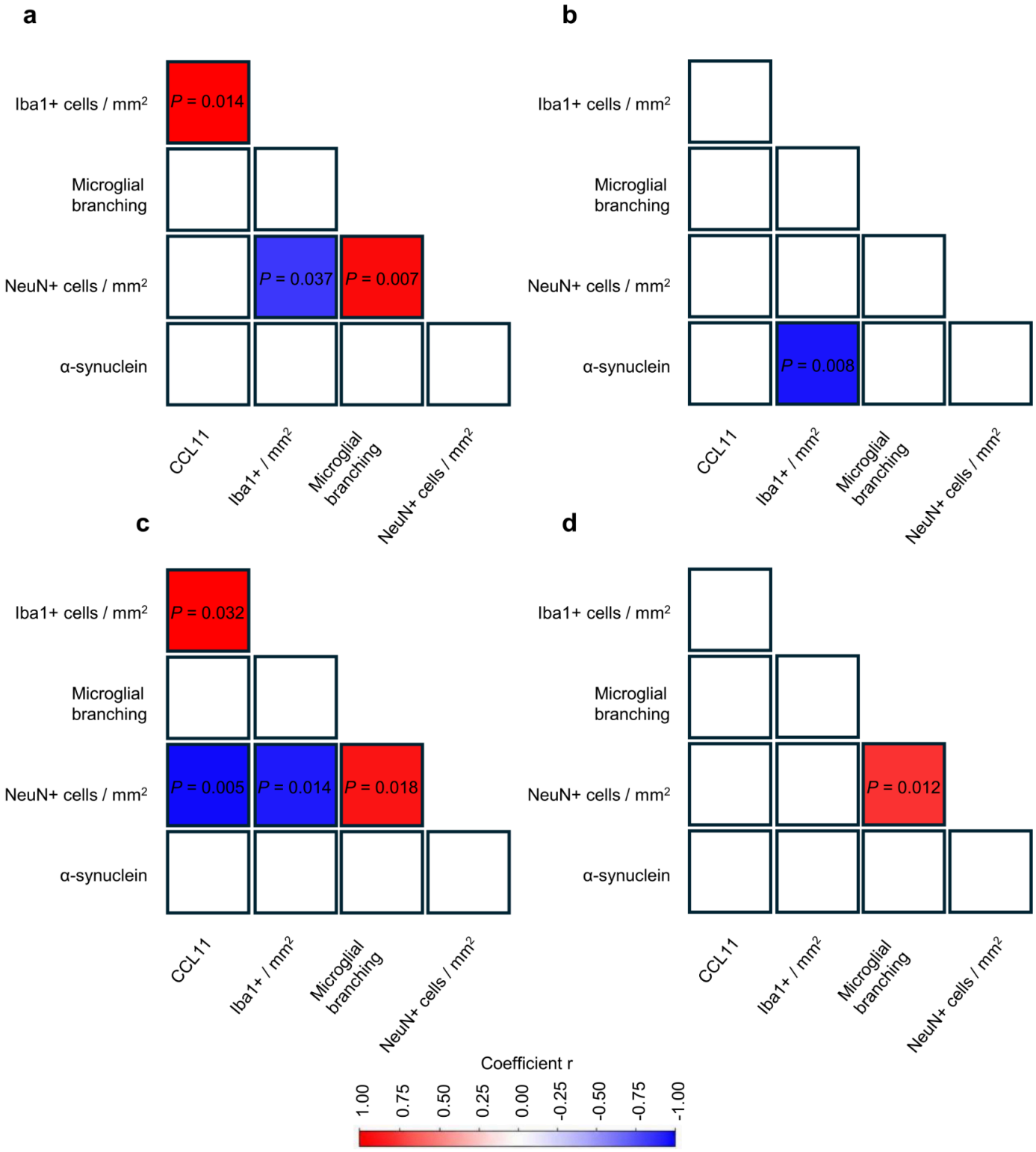


Figure 7

Correlation matrix showing the relationships among neuroinflammatory and neurodegenerative features in the hippocampus

(**a**) CA1 in females; **(b)**CA1 in males; **(c)** CA3 in females; and **(d)** CA3 in males. Microglial branching was assessed as the number of endpoints divided by the sum of branch lengths and then normalized to the number of Iba1$^+$ cells. Cells representing Pearson correlations with $P < 0.05$ are colored using a scale centered at zero

Supplementary Files

This is a list of supplementary files associated with this preprint. Click to download.

- ESM1.xlsx
- ESM2.xlsx